Al-Mustansiriyah Journal of Science
ISSN: 1814-635X (print), ISSN:2521-3520 (online) Volume 32, Issue 4, 2021 DOI: http://doi.org/10.23851/mjs.v32i4.1028

Research Article **Open Access**

Improvement of Corrosion Protection of Oil Pipeline Welding via Adding Tin Disulfide Nanoparticles

Atheer M. Jameel[1], Bahjat B. Kadhim[1,*], Fadhil K. Farhan[2]

[1]Department of Physics College of Science, Mustansiriyah University, Baghdad, IRAQ.
[2]Department of Medical Physics, College of Science, AL-Karkh University of Science, Baghdad, IRAQ.

*Correspondent contactl: sci.phy.bbk@uomustansiriyah.edu.iq

Article Info

Received
18/06/2021

Accepted
01/08/2021

Published
20/11/2021

ABSTRACT

The corrosion-resistant on the inner surface of the carbon pipeline welding alloys for two sections of the corrosion-resistant welding alloys (pure welding alloy) and welding alloys added Tin Disulfide Nanoparticles (SnS NPs) were welded by tungsten inert gas welding (TIG). The electrochemical behavior of the weld alloy was investigated at room temperature in 3.5% NaCl solution using potentiodynamic polarization. To reveal the corrosion resistance of alloys welded joints, some significant characterization parameters such as E_{corr}, I_{corr} and in polarization curves were analyzed and compared. The surface morphology of corrosion products was also analyzed by Scanning Electron Microscopy (SEM) and Atomic Force Microscopy (AFM) for two cases. The results show that the corrosion resistance for welding alloys added SnS Nps appeared high corrosion resistance, lower corrosion rate, and higher protection efficiency by 48% compared with pure welding alloy.

KEYWORDS: Corrosion; metal pipelines; carbon steel; welding; electrochemical.

INTRODUCTION

Corrosion is the performance degradation phenomenon of metals under the action of the surrounding medium [1, 2]. Carbon steel is widely employed in technical applications for equipment or construction materials, accounting for around 85% of yearly steel production worldwide [3].

Carbon steel is utilized in maritime applications, nuclear and fossil-fuel power plants, transportation, chemical processing, petroleum production and refining, pipelines, mining, building, and metal-processing equipment despite its low corrosion resistance [4]. Field pipelines are among the infrastructure that is most vulnerable to oil production. Although oil is not an aggressive medium in and of itself, the inclusion of salts, chlorine compounds, oxygen, hydrogen sulfide, and highly mineralized water in commercial oil products reduces pipe corrosion resistance. The presence of extremely abrasive particles in this substrate causes abrasive damage to appear and develop.

Corrosion and erosion problems significantly diminish the service life of oil field pipelines in Western Siberia, according to an analysis of actual service life. This service life may not always exceed one year [5]. Welding is widely used in the connection of oil /gas pipelines [6,7]. Therefore, it is necessary to protect the welding areas in these pipelines from the inside and outside, which leads to an improvement in corrosion resistance [8, 9]. Among the protection methods used in this field is thermal spray, as it is easy to apply [10].

For this, the chemical compounds used in the process of deposition of protective layers are made using ceramic materials and metals. Among the ceramic materials used in the coating are: Al_2O_3, TiO_2, ZrO_2, CaO and SnS as well as SnS_2 which is suitable with the use of the thermal spray method [11, 12, and 13].

Coating techniques are considered a recommended treatment for reducing the corrosion at the welded regions for the pipelines. The application of pipelines for various purposes is always related to the environment, such as air, water and soil. Each of these environments has different corrosively levels depending on ion concentration, temperature, relative humidity,

and solution resistance. For example, the NaCl content is different in solution [14]. Higher concentration of a solution will cause more hydrogen gas evolution. The stability of the halide in the surface complex determines the effect of corrosion kinetics of the metal/alloy according to Norio Sato [15].
the efficiency of corrosion techniques as the ASTM standard according to Tafel test are depended on the type of anode and cathode electrodes, electrolyte solution concentration and the path of electric charge transformation [16].
The aim of the present study is to investigate the corrosion behavior of Tin disulfide Nanoparticles added to welding alloy in 3.5 % NaCl concentrations by using Tafel polarization method.

MATERIALS AND METHODOLOGY

The ER 6010 is electrode wire use to welding the root pass for carbon steel pipes (CS) (A 106 grade B) was received from Ministry of Industry, Iraq. The chemical composition of as-received (CS) is given in Table 1. Tin disulfide type (SnS) was synthesized using wet chemical method under standard conditions. To get the (SnS) product, tin dichloride have the formula ($SnCl_2.2H_2O$) as the first source with sodium sulfide of the formula (Na_2S) as the second source for tin and sulfide are used respectively, with the present of deionized water which is used as solvent. The weight of ($SnCl_2.2H_2O$) was (12) g and for (Na_2S) was (18) g. The ($SnCl_2.2H_2O$) were dissolved in deionized water using magnetic stirrer for 2 hours at room temperature and (Na_2S) solution was dropping into the solution of $SnCl_2.2H_2O$). The precipitates (SnS) were washed with ethanol and dried in air at room temperature. According to this reaction (SnS) dark brown color nano powder were obtained.
Two models were prepared, the first model is (ER6010) wire weld joint and the third model is the ER6010 wire weld joint with SnS nanoparticles added using the gas tungsten arc welding GTAW process after removing the cellulose cover of the wire. Each model was divided into three parts (15x15) mm for doing the corrosion test. Before the samples were cleaned with acetone and then the samples were polished as per the metallographic procedure. The samples were polished with different SiC grit papers (400, 600, 800, 1000, 1200, 2000 SiC grits/in^2).
The Corrosion cell used in this research was made of Pyrex with a volume of (1) L constituting three electrodes. Samples were fixed in the NaCl solution at a concentration of 3.5 % was used to study the electrochemical test of ER6010 welded and (ER6010 welded+ SnS NPs) under the condition at room temperature.
Corrosion solution was attained by mixing 35 gram of NaCl pure and 1000 mL distilled water by use magnetic stirrer for 10 minute at room temperature to get NaCl 3.5%, as homogenous solution. Steel specimens were immersed in 1000 mL of 3% NaCl solution. The corrosion rate (*CR*), protraction efficiency (*PE* %) was determined using the following equations [17]:

$$Corrosionrate, CR = \frac{i_{corr}.K(EW)}{A.\rho} \quad (1)$$

Where *CR* is the corrosion rate, units are given by the choice of *K*. i_{corr} is the corrosion current in amps, *K* is a constant that defines the units for the corrosion rate (1.288×10^5 for mpy unit), *EW* is the equivalent weight of the specimen metal in grams/equivalent (27.92 g/equivalent), ρ is the density of the specimen metal in grams/cm^3 (7.87) for mild steel and A is the sample area in cm^2 [17].

$$PE\% = \left[\frac{i_{0corr} - i_{corr}}{i_{0corr}}\right] x100\% \quad (2)$$

Where, i_{0corr} and i_{corr} are the values of corrosion current density in the absence and presence of SnS NPs, respectively [18]. Polarization resistance measurements were used to obtain the polarization resistance (R_p) from the slope of the potential /current curve by using the fallowing equations [19]:

$$R_p = \frac{b_a \times b_c}{2.303 * (b_a + b_c).i_{corr}} \quad (3)$$

Where: b_a is slop1, b_c: is slop 2 and R_p: polarization resistance. The microstructural images in as-received condition and the worn surfaces were examined using the SEM (scanning electron microscope), with the AFM (atomic force microscopy).

RESULTS AND DISCUSSION

XRD diffraction patterns of synthesized (SnS) nanoparticles prepared by (Chemical method was conducted. The inter-planar spacing

measured were in good agreement with the spacing for the (110) (120), (111), (040), (041), (200), (141), (151), (122), (231), (042), (202), (023) and (133) planes for the orthorhombic SnS structure with JCPDS file NO. (00.039- 0354) as shown in the Figure 1. The most intense peak is at 32.08° corresponding to the plane (040). The size of the nanoparticles was estimated using Scherer's formula based on the full width at half-maximum (FWHM) of the different diffraction peak with different values [20]:

$$A = \frac{0.94\lambda}{\beta cos\theta} \quad (4)$$

Where: A is crystallite size, β is the FWHM of the diffraction peak, λ is the wavelength of X-ray radiation and θ is the angle of diffraction. The average Scherrer size of these NPs is 58.48 nm.

Force microscope gives good information about the surface topography. In addition to the statically determining the particles size from the 3D AFM images and granularity accumulation distribution chart of distribution, as shown in Figures 2, which is illustrate the AFM for model ER6010 welding alloy + (SnS) NPs. The root mean square quantity of the medium roughness of the surface (5.94) nm, the roughness average (5.04) nm, the mean size of the grain calculated is (71.12) nm.

Open circuit potentials (OCP) were carried out in electrolyte prior to run the electrochemical measurements. The specimens were immersed in the electrolyte (30 min) followed by (OCP) measurement for 30 min too.

The potentiodynamic polarization curves of the welding alloy and welding (alloy + SnS) NPs are illustrated in Figure 3 and Figure 4. The polarization was made by scanning the initial current from negative current (-10 mA) to final positive current (+10 mA) with the scan rate was 0.167 mA/s. The potentiodynamic polarization curves indicate that (E_{corr}) of welding alloy (–1.085 V) was relatively more positive than that of the (E_{corr}) of welding (alloy + SnS) NPs (–1.041 V). The anodic current density of welding alloy was higher than that of welding alloy + SnS NPs. The measured corrosion data of the two spaceman steels were determined as illustrated in Table 1 and 2 represent corrosion parameters which it calculates by Tafel curves.

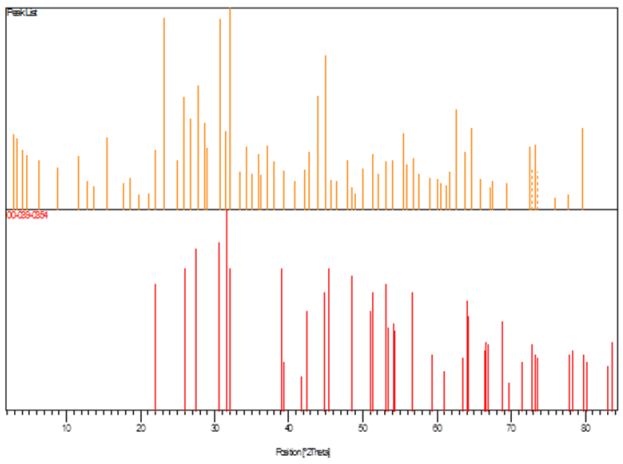

Figure 1. XRD identified Phases.

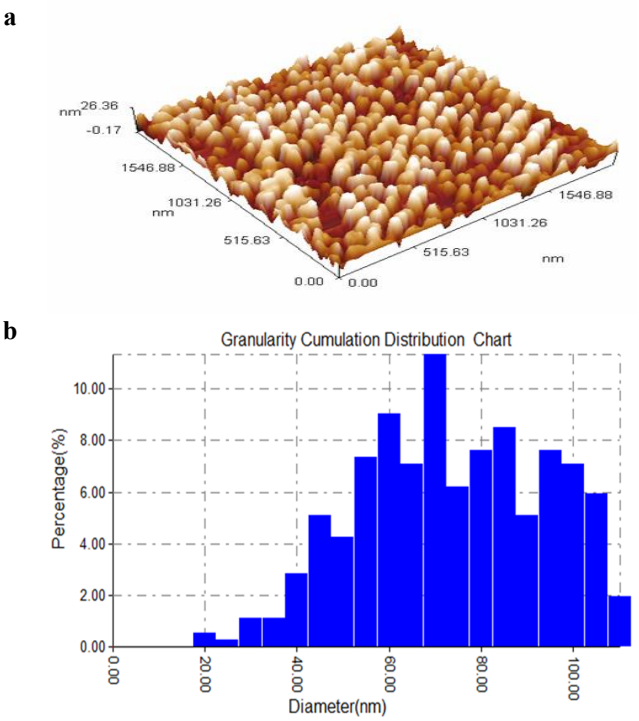

Figure 2. a) 3D AFM image ER6010 welding alloy+(SnS) NPs. B) Granularity accumulation distribution chart ER6010 welding alloy+(SnS) NPs.

Figure (5-a) illustrate the scanning electron microscopy (SEM) for welding alloy appears the surface is smooth and Figure (4-b) reveals that the model was highly corroded and appeared full of pits and cavities which may result from the aggressive attack of NaCl solution.

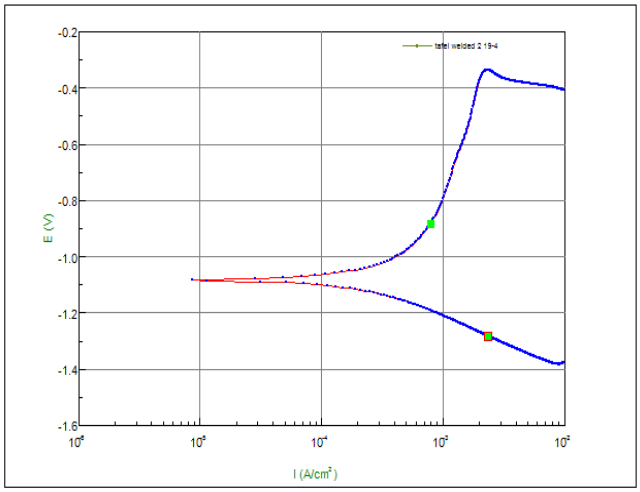

Figure 3. Tafel curve for welding alloy.

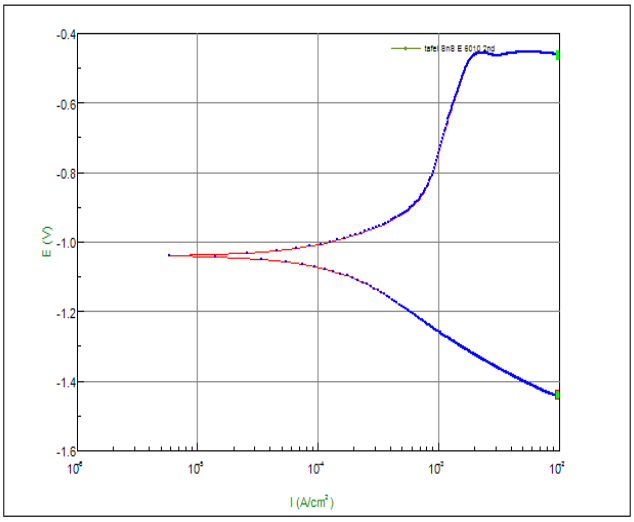

Figure 4. Tafel curve for welding alloy+SnS NPs.

Figure (5-a) shows the model welding alloy added SnS NPs before reaction. It is clear that the surface is smooth with some pits, cavities and scratches. The Figure (5-b) shows formation layer of film with some bumps appearing and some pitting covered which may result of the interaction of the NaCl solution with the Nanoparticles.

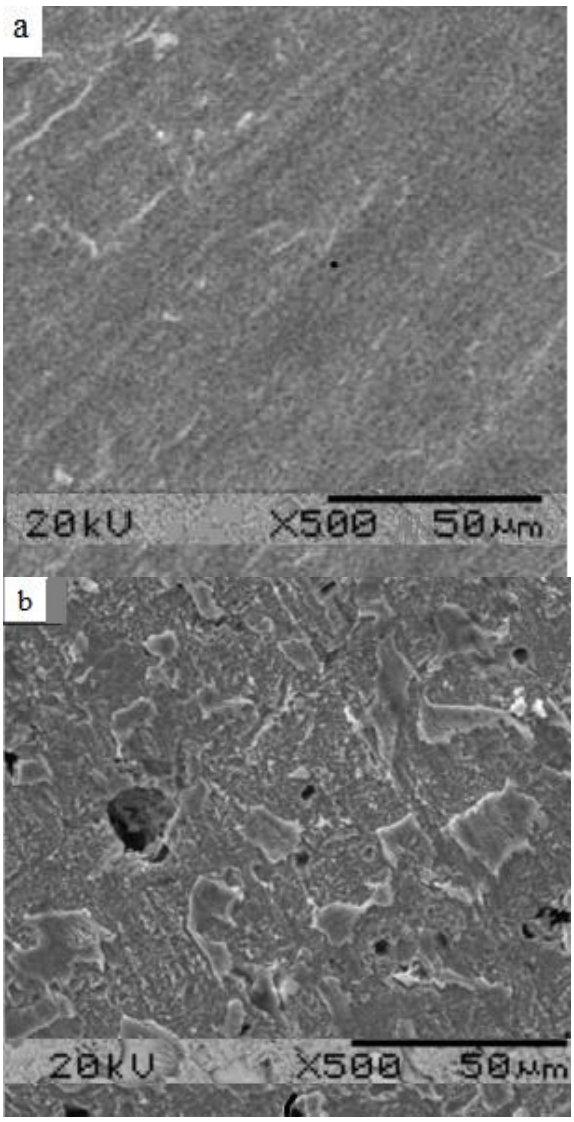

Figure 5. a) Welding alloy before reaction, b) Welding alloy after reaction.

Figure 6-a below shows the model welding alloy added SnS NPs before reaction. It is clear that the surface is smooth with some pits, cavities and scratches. The Figure 6-b shows formation layer of film with some bumps appearing and some pitting covered which may result of the interaction of the NaCl solution with the Nanoparticles.

Table 1. Corrosion data of specimens.

Specimens	E_{corr} (mV)	i_{corr} (µA/cm)	$-b_c$ (mV)	$+b_a$ (mV)
Welding alloy	-1.085	420.11	260.83	569.81
Welding alloy+(SnS) NPs	-1.041	216.77	343.43	295.11

Table 2. Corrosion parameters.

Specimens	Rp/Ω.cm^2	CR /mpy	CR /mm/y	PE%
Welding alloy	184.98	194.42	4.927	38.4
Welding alloy+(SnS) NPs	319.0	100.321	2.548	48.4

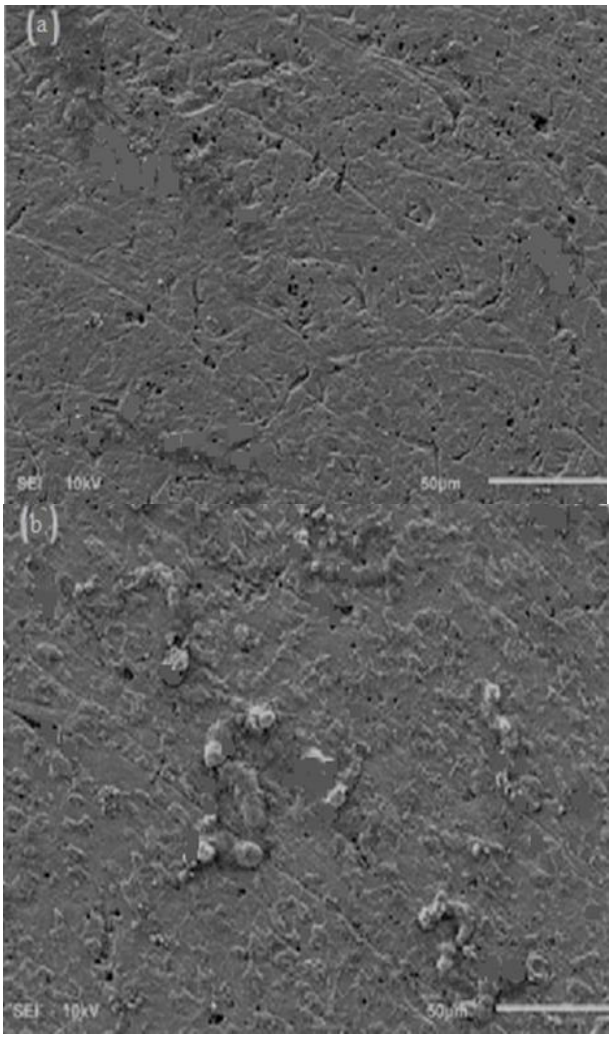

Figure 6. a) Welding alloy before reaction, b) Welding alloy after reaction.

CONCLUSIONS

The corrosion rate of the welding alloy added SnS NPs is lower than the corrosion rate value of the free welding alloy and more resistance to corrosion. Therefore, the SnS NPs are considered an inhibitor for corrosion. The SEM examination of worn surfaces shows that the SnS_2 nanoparticles added to the weld alloy reduce surface changing and at the higher the concentration, the more film builds up and the corrosion rate would be lower.

REFERENCES

[1] Jia, Ru, Tuba Unsal, Dake Xu, Yassir Lekbach, and Tingyue Gu. "Microbiologically influenced corrosion and current mitigation strategies: a state of the art review." International biodeterioration & biodegradation 137 (2019): 42-58.

[2] Wu, Tangqing, Maocheng Yan, Libao Yu, Hongtao Zhao, Cheng Sun, Fucheng Yin, and Wei Ke. "Stress corrosion of pipeline steel under disbonded coating in a SRB-containing environment." Corrosion Science 157 (2019): 518-530.

[3] Ismail, A., and N. H. Adan. "Effect of oxygen concentration on corrosion rate of carbon steel in seawater." American Journal of Engineering Research 3, no. 1 (2014): 64-67.

[4] Kadhim, Fadhil Sarhan. "Investigation of carbon steel corrosion in water base drilling mud." Modern Applied Science 5, no. 1 (2011): 224.

[5] Rodionova, I. G., O. N. Baklanova, E. T. Shapovalov, I. I. Reformatskaya, A. A. Podobaev, S. D. Zinchenko, S. V. Efimov, E. Ya Kuznetsova, L. A. Malyshkina, and A. V. Drandusov. "Methods of evaluating the corrosion resistance of low-alloy and carbon tube steels under the service conditions of oil and gas pipelines." Metallurgist 49, no. 5 (2005): 173-182.

[6] Cui, H. B., G. M. Xie, Z. A. Luo, J. Ma, G. D. Wang, and R. D. K. Misra. "The microstructural evolution and impact toughness of nugget zone in friction stir welded X100 pipeline steel." Journal of Alloys and Compounds 681 (2016): 426-433.

[7] Ye, Zheng, Jihua Huang, Zhi Cheng, Yufeng Zhang, Li Xie, Jian Yang, Shuhai Chen, and Xingke Zhao. "A novel high efficiency low heat input welding method: High frequency electric cooperated arc welding." Materials Letters 252 (2019): 142-145.

[8] Momber, A. W., and T. Marquardt. "Protective coatings for offshore wind energy devices (OWEAs): a review." Journal of Coatings Technology and Research 15, no. 1 (2018): 13-40.

[9] López-Ortega, A., J. L. Arana, E. Rodríguez, and R. Bayón. "Corrosion, wear and tribocorrosion performance of a thermally sprayed aluminum coating modified by plasma electrolytic oxidation technique for offshore submerged components protection." Corrosion Science 143 (2018): 258-280.

[10] Łatka, L., M. Szala, M. Michalak, and T. Pałka. "Impact of Atmospheric Plasma Spray Parameters on Cavitation Erosion Resistance of Al_2O_3-13% TiO_2 Coatings." Acta Physica Polonica, A. 136, no. 2 (2019).

[11] Czupryński, A. "Properties of Al_2O_3/TiO_2 and ZrO_2/CaO flame sprayed coatings." Spajanie Materiałów Konstrukcyjnych (2017).

[12] Szala, M., A. Dudek, A. Maruszczyk, M. Walczak, J. Chmiel, and M. Kowal. "Effect of Atmospheric Plasma Sprayed TiO_2-10% NiAl Cermet Coating Thickness on Cavitation Erosion, Sliding and Abrasive Wear Resistance." Acta Physica Polonica, A. 136, no. 2 (2019).

[13] Czupryński, A., B. Tomiczek, J. Górka, and M. Adamiak. "Testing of flame sprayed Al_2O_3 matrix coatings containing TiO_2." Archives of Metallurgy and Materials (2016).

[14] Ikechukwu, Anyanwu Samuel, Eseonu Obioma, and Nwosu Harold Ugochukwu. "Studies on corrosion characteristics of carbon steel exposed to Na_2CO_3, Na_2SO_4 and NaCl solutions of different concentrations." The International Journal of Engineering and Science (IJES) 3, no. 10 (2014): 48-60.

[15] Eddy, Nabuk Okon. "Green corrosion chemistry and engineering: opportunities and challenges." (2011).

[16] American Society for Testing and Materials. "Standard Reference Test Method for Making Potentiodynamic

Anodic Polarization Measurements: Designation: G5-13e1." ASTM, 2013.

[17] Sekunowo, O. I., S. O. Adeosun, and G. I. Lawal. "Potentiostatic polarisation responses of mild steel in seawater and acid environments." international journal of scientific & technology research 2, no. 10 (2013): 139-145.

[18] Behpour, M., S. M. Ghoreishi, N. Soltani, M. Salavati-Niasari, M. Hamadanian, and A. Gandomi. "Electrochemical and theoretical investigation on the corrosion inhibition of mild steel by thiosalicylaldehyde derivatives in hydrochloric acid solution." Corrosion Science 50, no. 8 (2008): 2172-2181.

[19] Clément, Antoine, S. Laurens, G. Arliguie, and F. Deby. "Numerical study of the linear polarisation resistance technique applied to reinforced concrete for corrosion assessment." European Journal of Environmental and Civil Engineering 16, no. 3-4 (2012): 491-504.

[20] Mousa, Fatin H., Ali S. Mahdi, Bahjat B. Kadhim, and Ali M. Ali. "Technological characteristics of perovskite solar cell windows using CdS–wurtzoid structure." In AIP Conference Proceedings, vol. 2190, no. 1, p. 020032. AIP Publishing LLC, 2019.